

Monolayers of polyethylenimine on flat glass: a versatile platform for cations coordination and nanoparticles grafting in the preparation of antibacterial surfaces†

Giacomo Dacarro,^{*a} Lucia Cucca,^b Pietro Grisoli,^c Piersandro Pallavicini,^{*d} Maddalena Patrini^a and Angelo Taglietti^d

Received 21st July 2011, Accepted 17th November 2011

DOI: 10.1039/c1dt11373a

A polyethylenimine (PEI) self-assembled monolayer (SAM) is prepared, capable of complexing silver and copper cations and of anchoring silver nanoparticles, exerting antibacterial activity against *Escherichia coli* and *Staphylococcus aureus*. Functionalized glassy surfaces have been fully characterized through spectroscopic techniques (UV-Vis spectroscopy, spectroscopic ellipsometry), atomic force microscopy imaging and quantitative Ag and Cu analysis (ICP optical emission spectroscopy).

Introduction

Nosocomial bacterial infections involving medical devices (e.g. prosthetics, catheters, implants) pose a serious challenge for biomedical researchers.¹ In the last twenty years great efforts have been made to prepare “smart” biomedical devices, capable of exerting a localized antibacterial activity.² We recently exploited the Layer-by-Layer (LbL) approach³ to prepare inorganic surfaces functionalized with silver nanoparticles (NP)^{4,5} and copper(II) complexes.⁵ We demonstrated that both silver NP and copper ions are firmly bound to the surface. Slow oxidation of NP surface and interaction with bacterial cells allow release of Ag⁺ and Cu²⁺ and a very high antibacterial activity against *Escherichia coli* and *Staphylococcus aureus* is observed, despite the small quantity of released metal cations. Surfaces coated with firmly grafted silver NP could be obtained with a thiol-terminated SAM^{3,4} formed on the bulk surface, but also by exploiting amine–silver bonds or electrostatic interactions. As regards the latter, amine–NP interactions have been widely studied and amino groups proved to be efficient coating and stabilizing agents for gold and silver nanoclusters.⁶ Amines can bind to the metal cluster surface through an electrostatic interaction^{6a} or a stronger

charge-neutral amine/metal interaction, described as a weak covalent bond.^{6d} Exploiting the same type of interactions, amine-terminated SAM have been used to anchor metal NP on surfaces.⁷ Amino propyl-silanes^{7a,7b} are a common choice for the preparation of amine-terminated monolayers, particularly on surfaces of SiO₂ type (glass, quartz, silica gel, etc.). Considering the enormously developed coordination chemistry of amino ligands, amines are to be considered a versatile moiety, since they can bind efficiently both NP and metal cations.

Polyethylenimines (PEI) are linear and branched polymers obtained by cationic polymerization of aziridine. Molecular weights of commercial PEI can vary in a very broad range, from a few thousands to hundreds of thousands g mol⁻¹. Commercial branched PEI typically have an amino group ratio primary:secondary:tertiary = 1:1:1.⁸ In solution, linear and branched PEI show good coordination properties towards various metal cations,⁹ typically displaying stronger affinity for M²⁺ transition metal cations.^{9d} Moreover, linear and branched PEI and similar polyamines have been used in a few papers as stabilizers and coating agents in metal nanoparticle synthesis.¹⁰

Layers of PEI on various surfaces have also been described. PEI can be grafted both exploiting weak electrostatic interactions between the polymer and inorganic surfaces^{11a} (e.g. glass, mica) or employing a silane-derivatized PEI (Scheme 1).^{11b,c} In the latter functionalization strategy, which has been only recently reported in literature, the polyaminic layer is covalently bound to the surface and is very stable as regards time and pH range.

With this background, silane-derivatized PEI appears as an ideal candidate for the preparation of organic monolayers on Si–OH terminated surfaces (glass, quartz, etc) to obtain multi-purpose materials. Continuing our investigation on surface-derivatized glass materials with antibacterial action, in this work we prepared a covalently bound SAM of PEI on glass-like

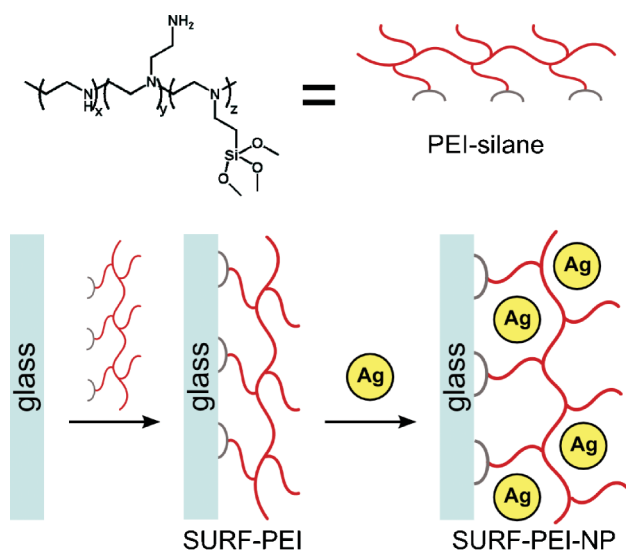
^aDipartimento di Fisica “A. Volta”, Università degli Studi di Pavia, Via Bassi 6, 27100, Pavia, Italy. E-mail: giacomo.dacarro@unipv.it; Fax: +39 0382 987563; Tel: +39 0382 987457

^bAnalytical Chemistry Section, Dipartimento di Chimica, Università degli Studi di Pavia, Viale Taramelli 12, 27100, Pavia, Italy

^cDipartimento di Scienze del Farmaco-Sezione di Farmacologia Sperimentale ed Applicata, Università degli Studi di Pavia, Viale Taramelli 14, 27100, Pavia, Italy

^dInorganic Nanochemistry Laboratory, Dipartimento di Chimica, Università degli Studi di Pavia, Viale Taramelli 12, 27100, Pavia, Italy

† Electronic supplementary information (ESI) available: ¹H-NMR spectrum of PEI-silane, SURF-PEI-NP pictures and background corrected UV-Vis spectra. See DOI: 10.1039/c1dt11373a



Scheme 1 Schematic representation of PEI-silane structure and two step synthesis of a Ag NP monolayer grafted on PEI SAM.

surfaces (*i.e.* glass, quartz, silicon with native SiO₂ overlayer) and we tested its coordination properties towards Ag⁺ and Cu²⁺. Moreover, we grafted a layer of silver NP on the polyaminic SAM. In both cases, we wished to prepare a surface capable of a modulated release of silver cations avoiding a potentially risky release of metallic nano-objects in the medium. The monolayers were characterized by means of optical spectroscopies (UV-Vis, spectroscopic ellipsometry) and the morphology of the SAM was verified with Atomic Force Microscopy (AFM) imaging. Total quantities of silver and copper loaded on the surface and their release in water were determined by means of inductively coupled plasma optical emission spectroscopy (ICP-OES). The antibacterial activity of the functionalized glasses was tested against *Escherichia coli* and *Staphylococcus aureus*, finding an efficient microbicidal effect.

Experimental

Materials

Silver nitrate (>99.8%), sodium borohydride (>99.0%), sodium citrate (>99.0%), fluorescein-isothiocyanate (FITC, >90%), copper trifluoromethanesulfonate (98%), silver trifluoromethanesulfonate (>99%) and PBS were purchased from Sigma-Aldrich. Trimethoxysilylpropyl(polyethylenimine) (50% in isopropanol) was purchased from Gelest Inc. Reagents were used as received. Solvents were purchased from Sigma-Aldrich and used as supplied. Microscopy cover glass slides (2.4 × 2.4 cm) were purchased from Forlab (Carlo Erba). Quartz slides (Spectrosil 2000 fused silica, 1.4 × 1.4 cm, 1 mm thick) were purchased from UQGOptics Ltd. Water was deionized and then bidistilled. Silver NP (average diameter $d = 7$ nm, $\sigma = 4$ nm) were prepared as described in ref. 4.

CuPEI and AgPEI complexes spectrophotometric characterization

A solution of PEI-silane in ethanol (2.1×10^{-4} M) was titrated with a 0.104 M solution of copper trifluoromethanesulfonate in ethanol, by repeated additions of substoichiometric, few microlitres volumes of Cu²⁺ to 20.0 mL of the PEI-silane solution, at 20 °C, under

a N₂ atmosphere. Absorbance spectra were recorded in the 200–1100 nm range. A titration with silver trifluoromethanesulfonate was performed under the same conditions. Trifluoromethane counter ion was chosen for its non-coordinating properties and because its metal salts can be easily obtained in an anhydrous form.

Preparation of PEI-silane self-assembled monolayers on glass surface (SURF-PEI glasses)

PEI monolayers were prepared according to ref. 11b, with minor alterations. Briefly: glass and quartz substrates were cleaned for 30 min in freshly prepared Piranha solution (3 : 1 v/v H₂SO₄:H₂O₂ (30%). *Caution! Piranha solution is a strong oxidizing agent and should be handled with care.*, washed three times with ultrapure water in a sonic bath and oven-dried. The slides were then immersed for 6 min in a 2% (v/v) solution of PEI-silane in ethanol at room temperature. In a typical preparation, 8 glass slides were prepared at the same time, *i.e.* reacting in the same silane solution inside a 8-place holder (a microscope glass slides staining jar). After this, the slides were washed three times with ethanol and one time with ultrapure water in a sonic bath and blow-dried with nitrogen. Functionalized glasses were left to cure overnight at room temperature before use.

FITC modification of PEI monolayers

SURF-PEI functionalized glasses were immersed in a 2.6×10^{-4} M FITC solution in CH₃CN (100 μl triethylamine was added to the solution) for 4 h at room temperature, as previously reported for the functionalization of a similar amino terminated SAM.¹² Glass slides were then washed three times with CH₃CN in a sonic bath and blow dried with nitrogen.

Cu²⁺ and Ag⁺ complexation in PEI monolayers

SURF-PEI functionalized glasses were immersed in a 10⁻³M solution of the proper trifluoromethanesulfonate metal salt in CH₃CN for 4 h. Glass slides were then washed three times with CH₃CN in a sonic bath and blow dried with nitrogen.

Silver nanoparticle monolayer preparation

SURF-PEI glasses were immersed in the colloidal suspension of citrate-capped silver NP⁴ at room temperature for different times (from 15 min to 18 h). In a typical preparation, 8 glass slides were prepared at the same time, *i.e.* they were made to react in the same NP suspension, inside a glass holder (where the slides were kept in vertical position). After this, the obtained glasses (showing a yellow to red colour, depending on immersion times) were placed in water and sonicated for 5 min. This procedure was repeated twice and then the glasses were blow dried with a nitrogen stream and stored in the dark.

Antibacterial activity tests

The antibacterial activity of functionalized cover glasses was investigated against *Staphylococcus aureus* ATCC 6538 (Gram+) and *Escherichia coli* ATCC 10356 (Gram-). The microorganisms were grown overnight in Tryptone Soya Broth (Oxoid; Basingstoke, Hampshire, England) at 37 °C. Washed cells were resuspended

in Dulbecco's PBS and optical density (OD) was adjusted to 0.2 at 650 nm wavelength, corresponding approximately to 1×10^8 Colony Forming Units (CFU)/ml. 10 μ l of bacterial suspension was deposited on a standard glass slide (76 \times 26 mm), then the microbial suspension was covered with a functionalized cover glass slide (24 \times 24 mm), forming a thin film between the slides that facilitates direct contact of the microorganisms with the active NP surface. The two assembled glasses were introduced in a Falcon test-tube (50 ml) containing 1 ml of PBS to maintain a damp environment. In this test microbes are incubated in non-nutritive suspensions that do not give the microorganisms the potential to grow during the test. For each bacterial strain two equivalent modified glasses were prepared; the slides were maintained in contact with the liquid films containing bacteria at room temperature for 5 and 24 h, respectively; for each time of contact an unmodified glass slide was treated in the same way as control sample. After the times of contact, 9 ml of PBS were introduced in each Falcon test-tube under a gentle shaking to detach the assembled glass slides. Bacterial suspensions were then grown in Tryptone Soya Agar (Oxoid; Basingstoke, Hampshire, England) to count viable cells. The decimal-log reduction rate, *i.e.* the Microbicidal Effect (ME), was calculated using the formula:

$$ME = \log N_C - \log N_E$$

(N_C being the number of CFU/ml developed on the unmodified control glasses, and N_E being the number of CFU/ml counted after exposure to modified glasses). The results expressed as ME represent the average of three equivalent determinations.

This method can be considered as a version of the Japanese Industrial Standard JIS Z 2811 developed to measure the antibacterial activity of plastic surfaces.

Instrumentation and instrumental methods

Absorbance spectra of colloidal suspensions and metal complexes solutions were taken with a Varian Cary 100 spectrophotometer in the 200–900 nm range or with a HP8453 diode array spectrophotometer in the 200–1100 nm range. Spectra of functionalized glasses or quartzes were obtained placing the slides on the Varian Cary100 spectrophotometer equipped with a dedicated Varian solid sample holder.

NMR spectra (400 MHz) were taken on a Bruker AMX400 instrument.

Contact angle determinations were made with a KSV CAM200 instrument, with the water sessile drop method.

AFM images were taken from an Auto Probe CP Research Thermomicroscopes scanning system in tapping mode with Au coated Si probe with a theoretical spring constant $k = 2.5$ – 10 Nm^{-1} (NSG01 probes from NT-MDT). Images were analyzed using Image Processing 2.1 provided by Thermomicroscopes.

Ellipsometric spectra were measured from 0.25 to 0.9 μ m with an automatic SOPRA ES4G rotating polarizer ellipsometer, equipped with a single-photon-counting photomultiplier detector, at angles of incidence of 70 and 75 degrees. Experimental results were analyzed with the WVASE32 software from J.A. Woollam Inc. Ellipsometric analysis was performed on naturally oxidized silicon samples, prepared with a procedure identical to that applied to the glass slides.

The total Ag content on glasses with NP monolayers was determined by quantitatively oxidizing the silver NP grafted on a single slide (24 \times 24 mm or 12 \times 24 mm) by dipping it in 5 ml ultrapure concentrated HNO_3 diluted 1 : 5 with water (13% w/v as final concentration) in a vial, and keeping it overnight at RT on a Heidolph Promax 1020 reciprocating platform shaker. The Ag content in solution was then determined by inductively coupled plasma optical emission spectroscopy (ICP-OES) with an ICP-OES OPTIMA 3000 Perkin Elmer instrument.

Results and discussion

Study of PEI complexes in solution

Literature reports that on addition of Cu^{2+} ions, PEI forms a blue copper-amine complex, with a d–d absorption band in the 610–640 nm region of the visible spectrum. A LMCT band is also present in the UV region, with a maximum at 270–290 nm. The position of the absorption bands depends on the N:Cu ratio of the complex, which can vary from 4 : 1 to 6 : 1, according to literature.¹³ Commercial PEI-silane (MW 2000–4000) was titrated with Cu(II) and Ag(I) to check its coordination properties towards the two cations, using a $2 \times 10^{-4} \text{ M}$ solution of PEI-silane in ethanol and trifluoromethanesulfonate salts.

As regards Cu(II), our main goal was to assess the stoichiometry of the complex in solution, *i.e.* the number of Cu^{2+} ions that each PEI polymer is able to bind. The Cu–(PEI-silane) complex shows two absorption bands, as expected, centered at 274 nm and 636 nm with molar absorptivities of $\epsilon_{274} = 4330 \text{ cm}^{-1}\text{M}^{-1}$ and $\epsilon_{636} = 230 \text{ cm}^{-1}\text{M}^{-1}$, respectively (ϵ referred to the Cu^{2+} ion). The former is a LMCT band while the latter is the typical d–d transition involving tetragonally distorted Cu^{2+} with sterically encumbered ligands (*e.g.* for $[\text{CuL}_2]^{2+}$, $\lambda_{\text{max}} = 587 \text{ nm}$ in water for $\text{L} = \text{H}_2\text{N}-\text{CH}_2-\text{CH}_2-\text{N}(\text{Et})_2$ and 634 nm at the solid state for $\text{L} = (\text{Et})\text{HN}-\text{CH}_2-\text{CH}_2-\text{NH}(\text{Et})$).¹⁴ The large shoulder between 700 and 1100 nm (Fig. 1a) is indicative of a mixture of Cu^{2+} coordinative environments, with some cations arranged in a trigonal-bipyramidal fashion, as in *e.g.* $[\text{Cu}(\text{tren})]^{2+}$ ($\text{tren} = 2,2',2''$ -triaminotriethylamine), that is a typical five-coordinate complex with λ_{max} in the 790–820 nm range.¹⁵ After an absorbance plateau is reached, a further absorbance increase in the 800–1000 nm region is due to excess Cu^{2+} that remains free in solution as its solvation (see spectrum in ESI†). As it is shown in Fig. 1a, inset, each molecule of PEI-silane is able to bind 12 Cu(II) cations (corresponding to a 25% metal doping).

The commercial PEI-silane structure, pictorially depicted in Scheme 1, has been investigated by $^1\text{H-NMR}$ (see ESI†). From the ratio of the integrals of the peaks associated to the different methylene protons, we determined a 15.65 : 1 ratio between ethylamino monomers of the PEI and propyl-silane moieties, corresponding to an average of 3.6 propyltrimethoxysilane groups on each polymer. From this value it was possible to estimate that each PEI-silane contains 56 ethylenimine monomers, *i.e.* 56 amine moieties (including primary, secondary and tertiary amines). By combining NMR and absorbance data, a N:Cu ratio of 4.7 is calculated, which is in good agreement with the 4–6 range reported in literature¹³ and with the qualitative observations on spectral absorbance.

Polyamines (*e.g.* linear and branched tetramines) are also capable to bind Ag(I) ions, but it has been reported that the formation of

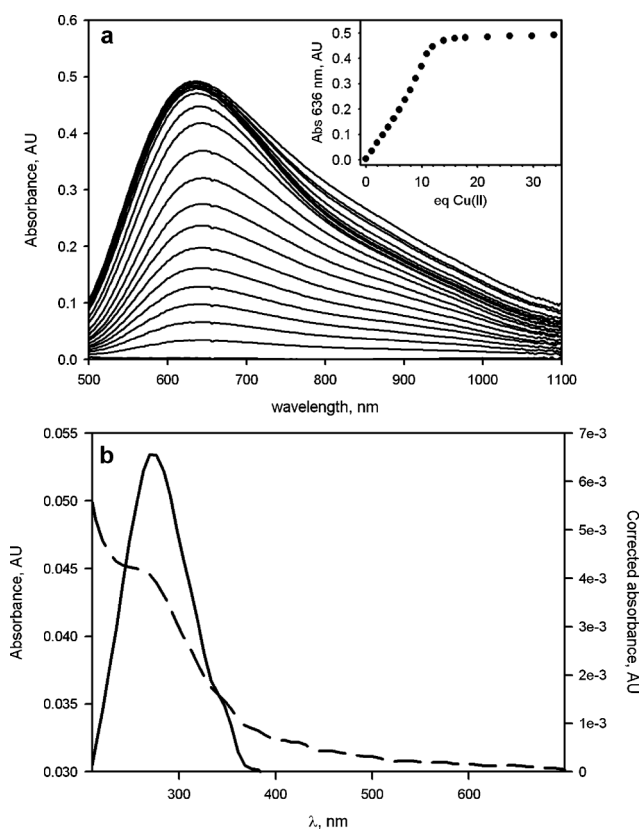


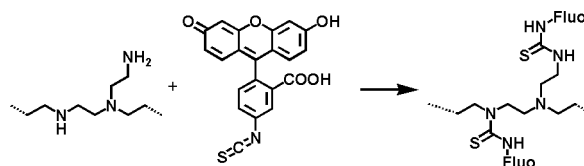
Fig. 1 (A) d-d absorption band increase in PEI-silane titration. Increasing amounts of Cu(II) were added to an ethanolic PEI-silane solution. Inset shows the titration profile of absorbance at 636 nm vs. added Cu(II): a plateau is reached upon addition of 12 equivalents. (B) UV-Vis spectrum of SURF-PEI after complexation with Cu(II) (dashed spectrum, absorbance on left axis). The solid line spectrum (absorbance on right axis) is obtained by background subtraction.

the complex cannot be followed *via* spectrophotometric titration, due to the absence of significant spectral changes in the UV-Vis region.¹⁶ Being Ag⁺ a d¹⁰ cation, neither d-d nor LMCT bands are formed with amino ligands, and Ag-polyamine complexes do not show any variation in the absorbance spectra, as we verified in our case with a titration of the PEI-silane with silver trifluoromethanesulfonate (data not shown). However, it can be expected that the used molecule have non-negligible binding properties towards Ag(I), at least comparable to those described in literature for polydentate polyamino ligands like **tren** and **trien** (1,4,7,10-tetraazadecane). Logarithmic binding constants in water (with 1:1 stoichiometry) for these ligands are 7.7^{16a} and 7.5,^{16b} respectively.

Preparation of SURF-PEI on glass

We grafted PEI-silane molecules on glassy surface by a quick, straight-forward procedure reported in literature,^{11b} forming a monolayer. Glass or quartz slides were cleaned and activated with a strong acidic and oxidizing solution, obtaining a highly hydrophilic surface (contact angle <10°). Activated surfaces react quickly with an ethanolic solution of PEI-silane. Each polymer molecule has multiple attaching points: as we discussed in the previous paragraph, an average of 3.6 silane moieties/polymer

are present in the used PEI-silane. PEI-functionalized surfaces showed a static contact angle of 41 ± 5° on glass, 41 ± 7° on quartz and 43 ± 2° on silicon (values are an average from 8 samples, 4 measurements were performed on each sample on different spots). Obtained values are in good agreement with the value of 44 ± 2° reported in literature for functionalized silicon surfaces.^{11b} To estimate the number of reactive primary and secondary amino groups on the SAM we carried out a coupling reaction with fluorescein-isothiocyanate (FITC), similarly to what we reported for the evaluation of surface thiol groups with tetramethylrhodamine-maleimide.¹⁷ PEI modified glass slides were made to react with a FITC solution following a literature protocol,¹² by the formation of thiourea moieties from the reaction of R-NH₂ or RR'NH PEI amines with R''-N=C=S (Scheme 2). Surface concentration *n_s* of the chromophores (*i.e.* surface concentration of reactive amines) was determined using Lambert-Beer equation, modified for the case of a two-dimensional sample:¹⁷ $n_s(\text{cm}^{-2}) = 6 \times 10^{20} A/2\epsilon$, where *A* is the absorbance measured on functionalized surface, ϵ is the molar absorptivity of FITC in solution ($\epsilon_{492\text{ nm}} = 77000 \text{ cm}^{-1}\text{M}^{-1}$) and the factor 2 is needed since the slides are functionalized on both sides). Averaging 20 experiments (5 different preparations of 4 glasses each) we obtained $n_s = 5.0 \times 10^{13} \text{ cm}^{-2}$. This value is reasonable even if it is lower with respect to what we obtained for a glass surface coated with mercaptopropyltrimethoxy silane (MPTS), *i.e.* a surface bearing a thiol monolayer capable of coupling with functionalized dyes ($n_s = 1.4 \times 10^{14} \text{ cm}^{-2}$).¹⁷ However, we must take into account that tertiary amines do not react with isothiocyanates and secondary amines may have a lower reactivity and be sterically hindered, especially if we consider a monolayer of a flexible polymer like PEI, grafted to a bulk surface.



Scheme 2 Reaction of PEI primary and secondary amines with FITC.

Using UV-Vis absorption spectroscopy on glass slides we investigated also the formation of Cu(II) complexes on SURF-PEI, by monitoring the charge transfer band in the UV region. To avoid saturation, spectra were recorded on quartz slides (Spectrosil 2000 fused silica, internal transmission >99.9% at 248 nm) and corrected for the background^{17,18} (Fig. 1b). The *n_s* values were calculated using $\epsilon_{274} = 4330 \text{ cm}^{-1}\text{M}^{-1}$ (obtained from Cu(II) complex of PEI-silane in solution). Averaging the results of five samples, we obtained $n_s(\text{Cu(II)}/\text{cm}^2) = 2.3 \pm 1.6 \times 10^{14} \text{ cm}^{-2}$, which is of the same order of magnitude previously reported for the coating of glass surfaces with trialkoxysilanes.^{17,19} Moreover, this value is also comparable to what we obtained for a SAM made of a silane-functionalized macrocyclic copper(II) complex.⁵ The concentration of Cu(II) on the SAM was also directly measured by demetallating the coated glass slides with 2% v/v HNO₃ (48 h) and measuring the total copper content in solution with inductively coupled plasma optical emission spectroscopy (ICP-OES). We found $1.8 \pm 0.2 \times 10^{14} \text{ cm}^{-2}$, a result in good agreement with optical data showed above. It has to be noted that NMR and UV-Vis titration in solution led us to calculate that an average ratio of

4–5 N:Cu is obtained for fully binding PEI. On the other hand, the determination of primary and secondary amines with FITC coupling yielded a value that is ~ 3 times lower than that found for Cu^{2+} content, this strongly points towards the poor accessibility and/or decreased reactivity towards FITC of secondary (and possibly in part primary) amino groups for surface-grafted PEI.

SURF-PEI was also loaded with Ag(I) ions, following the same preparation protocol used for Cu(II) loading. In this case, complexation cannot be followed with UV-Vis spectrophotometric measurements, as it has already been noted in solution. Surface concentration of Ag ions was determined by ICP-OES. We found $n_s(\text{Ag}/\text{cm}^2)$: $3.8 \pm 0.5 \times 10^{13} \text{ cm}^{-2}$, corresponding to the 20% of the concentration determined for Cu ions. This is predictable considering the lower binding constants of polyamines toward Ag(I), with respect to Cu(II).

Contact angle measurements on glasses loaded with Cu(II) and Ag(I) showed no significant variations with respect to **SURF-PEI**: average static water contact angles were $47 \pm 3^\circ$ and $42 \pm 3^\circ$ for 8 samples loaded with Cu and Ag ions, respectively.

AFM images have been taken on a bare glass slide, on a sample functionalized with PEI and on Cu(II) and Ag(I) loaded samples. Different areas with lateral size ranging from $5 \mu\text{m}$ to 250 nm were examined. The surfaces appear flat and homogeneous and rms roughness values are very low. Roughness decreases slightly after functionalization with PEI-silane (rms value = $0.15 \pm 0.02 \text{ nm}$) with respect to the clean glass slide ($0.19 \pm 0.07 \text{ nm}$). Complexation with Cu(II) ions produces a small increase in roughness ($0.26 \pm 0.03 \text{ nm}$) while Ag(I) complexation did not induce a significant change.

The same silicon wafers used for AFM imaging were characterized also by means of spectroscopic ellipsometry to assess the thickness of the SAM. From the best fit on spectroscopic ellipsometry (SE) spectra an effective layer growth of $0.25\text{--}0.45 \text{ nm}$ was found, using a literature dielectric function for PEI.²⁰ Although we cannot predict precisely the conformation of the PEI polymer in the layer, we can expect each polymer molecule to be grafted in several points per polymer on the surface, as we estimated by NMR the presence of 3–4 $\text{Si}(\text{OCH}_3)_3$ moieties on each polymer molecule. This favours a flat conformation, that may be also promoted by $-\text{NH} \cdots \text{O}(\text{Si})$ interactions, which have been already described for silica-grafted amines,²¹ leading to a low organic layer thickness. In this case, the use of the term “self-assembled monolayer” could be misleading. Usually the term SAM refers to ordered systems, formed by small molecules closely packed on a flat surface. Moreover, we note that the values reported are effective thicknesses that should be significantly lower than the actual layer thickness when accounting for the presence of a void fraction. SE measurements performed after Cu(II) and Ag(I) complexation on the SAM did not produce a significant variation in layer thicknesses.

To assess the stability of metal ion complexation we carried out a release test in water, measuring the concentration of released cations in solution after 24 h. As we reported previously for the case of a macrocyclic copper complex monolayer,⁵ both Ag and Cu complexes released a very small quantity of metal cations ($< 5\%$, very close to the detection limit of ICP-OES instrument).

NP grafting

Grafting of silver NP was obtained by dipping the glass slides bearing **SURF-PEI** in aqueous colloidal suspensions of citrate-

capped Ag NP, prepared according to a standard method.⁴ Spectra of silver nanoparticles grafted on PEI-modified glasses were recorded in air, after drying the slides with a nitrogen stream. On increasing dipping times, the slides showed an evident change in color, from yellow (typical for non interacting, small spherical silver NP) to red and brown-black (see ESI†). UV-Vis absorbance spectra displayed huge variations in the intensity and line shape of the surface plasmon resonance (SPR) band related to the particles. However, as it can be seen in Fig. 2, glass slides have a non negligible absorption in the visible and UV regions of the spectrum, which can interfere with a correct determination of the peak's position (λ_{max}), intensity and width (FWHM, full width at half maximum). The absorbance spectra were thus analyzed using a home-made software, that allows to interpolate the background with a cubic spline and to subtract it from the experimental curves, as already reported in the literature.^{17,22} From the normalized spectra, the correct parameters of the absorbance peaks can be accurately determined. All the values mentioned in the paper are taken from normalized spectra unless otherwise stated.

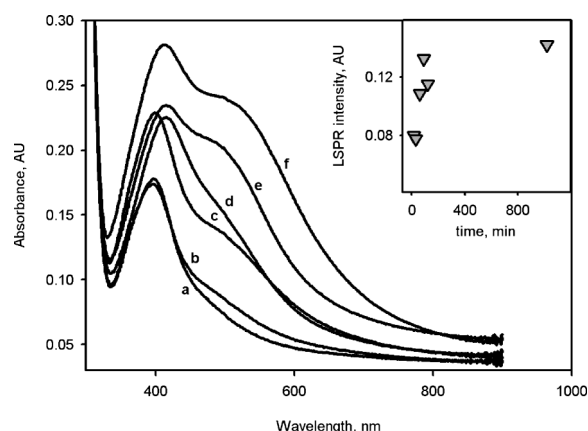


Fig. 2 UV-Vis absorbance spectra as a function of dipping time (a: 15 min, b: 30 min, c: 60 min, d: 90 min, e: 120 min, f: 18 h) on **SURF-PEI-NP** modified glasses. Inset shows the variation of LSPR intensity vs. time. Intensity values are from background subtracted spectra. Three spectra on different spots of the same sample were taken and average values were plotted. LSPR intensity is calculated at the wavelength of maximum absorption of each spectrum, ranging from 400 nm to 420 nm.

Fig. 2 shows a typical series of uncorrected UV-Vis spectra recorded for PEI-functionalized glasses that were dipped in a NP suspension for different times (ranging from 15 min to 18 h; corrected spectra are provided in ESI†). For short immersion times (15 min, spectrum **a** in Fig. 2) the SPR band is symmetric and centered at a $\lambda_{\text{max}} = 403 \text{ nm}$ (*vide infra*), a value comparable to what was reported previously⁴ for similar particles on thiol-terminated SAM (398 nm). A small but significant shift is observed for the SPR with respect to Ag NP dispersed in solution (SPR at 394 nm). The shift has to be attributed to the change in the NP environment, *i.e.* solvent refraction index²³ and the coating agent on the NP surface. For longer immersion times (from 30 min to 18 h, spectra **b–f**, Fig. 2) we observe a red shift of the SPR band and a significant peak broadening, leading to the formation of a shoulder on the band, centered at about 510–520 nm. Moreover, an increase in the peak intensity is also observed at long dipping times. AFM imaging at 15 min dipping time (Fig. 3a) showed the

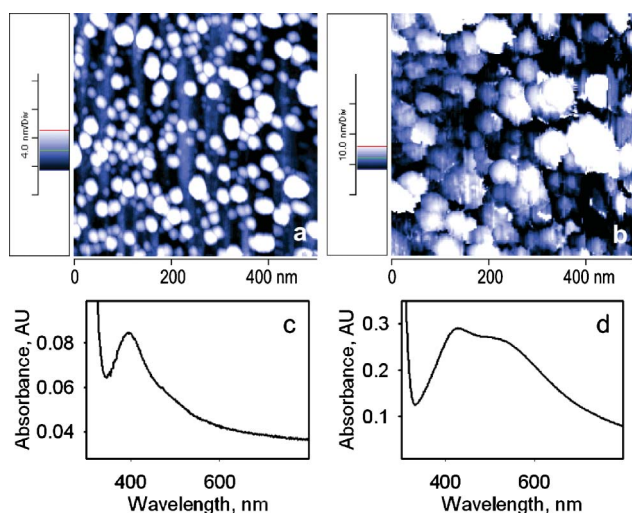


Fig. 3 (a,b) AFM topography images (500×500 nm) of SURF-PEI-NP modified glass slides prepared at 15 min (a) and 18 h (b) dipping times. (c,d) UV-Vis spectra of the same slides (c: 15 min, d: 18 h dipping time).

typical monolayer structure observed for the same NP grafted on thiols⁴ or on copper complexes SAM.⁵ On the other hand, AFM imaging on slides dipped for longer time showed an enlargement of the apparent NP diameter (Fig. 3b). The SPR red-shift and enlargement are clearly connected to the NP morphology change, as it is shown by the corresponding absorbance spectra (Fig. 3c–d). Total Ag quantities were determined for these samples by means of ICP-OES spectroscopy, showing an increase of loaded metal as a function of immersion time (*vide infra*).

It has however to be stressed that at dipping times ≥ 30 min reproducibility is poor. Variations of the absorption spectra and of surface morphology of NP layers have always similar trends, but SPR line shape and position (as well as average dimensions of NP determined by AFM), taken at a chosen time, may vary significantly and unpredictably from one preparation to another.

Due to this, we decided to focus our studies on glasses functionalized with PEI SAM and NP at short immersion times (*i.e.* 15 min), that showed a good reproducibility. These were fully characterized, by means of UV-Visible spectroscopy, AFM, spectroscopic ellipsometry and ICP-OES. The mentioned 403 nm value for SPR peak comes from 40 analyzed samples, and bears a standard deviation of ± 3 nm. Intensity is 0.05 ± 0.02 in absorbance units and FWHM of 87 ± 20 nm.

The deviation in the SPR position with respect to an aqueous dispersion of the same NP has been already commented. Similar considerations apply when comparing these results to those found using a thiol-terminated MPTS SAM for adhesion of the same (citrate-capped) nanoparticles, *i.e.* SPR = 398 ± 4 nm.⁴ This small difference can be related either to the different type of adhesive molecular monolayer and to the different organic layer–NP interactions, or to the fact that, in the present case, Ag–NP may be fully included and hidden in the PEI layer, while in the case of grafting on MPTS almost 65% of the NP surface remains directly exposed to solvent.⁴

Total Ag quantity loaded on glasses was measured by means of ICP-OES, quantitatively oxidizing the NP on functionalized glasses and analyzing the obtained solutions. We found a surface

concentration of $7.6(\pm 1.2) \times 10^{-7}$ g cm⁻² of Ag.[‡] An Ag sphere of 7 nm diameter has a 1.897×10^{-18} g mass. The mass/cm² data from ICP-OES correspond thus to a count of 4.0×10^{11} silver NP/cm². This value is considerably higher if compared to what we observed for a NP layer on a thiol-terminated SAM, *i.e.* 1.9×10^{11} NP/cm².¹⁷ AFM imaging (Fig. 3a), however, shows for our NP on PEI the same morphology as for Ag NP on a MPTS adhesive SAM.⁴ On a 500×500 nm window we counted 282 NP, which would lead to a lower quantity of grafted Ag NP (1.1×10^{11} NP/cm²) with respect to what found with ICP-OES analysis. Considering the morphology of the particles showed by the AFM images we can rule out aggregation or changes in NP shape in the 15 min dipped samples. The measured NP height, which gives a correct indication of the particle size, is 6.0 ± 1.6 nm, compatible with a diameter of 7 ± 4 nm, measured with Transmission Electron Microscopy.^{4§} To explain the larger quantity of Ag found by ICP-OES we hypothesize that the polymeric, branched nature of PEI allows the formation of a NP multilayer (see Scheme 1), instead of a monolayer as with MPTS. Coated glass slides thus present the same surface morphology to the AFM tip, but more NP are placed under the surface, in the PEI layer. This hypothesis is fully confirmed by SE measurements, carried on a SiO₂-coated wafer, that underwent the same functionalization procedure we applied to glass. The SE spectra gave a clear evidence of the SPR absorption band of silver NP, that was simulated by a Gaussian-like dielectric function. Best fit of SE data showed a layer thickness of 10–14 nm, indicative of a double layer of particles. It must be stressed that these layers are made of distanced nanoparticles,^{4,5} as confirmed by AFM imaging and SPR lineshape.[¶] We can thus suppose that, also in the presence of a double layer, NP are not exactly superimposed, but randomly distributed at a distance at which they do not interact.

Ag release from functionalized glasses was measured from samples dipped in ultrapure water and shaken for 14 days. Concentration of Ag⁺ in the resulting solutions was measured by means of ICP-OES spectroscopy: NP functionalized glasses released on average the 8.2% of grafted Ag during the same period. The percentual quantity of released Ag is lower with respect to what we found for NP grafted on thiol-terminated SAM.⁴ However, the absolute Ag⁺ quantities released in solution are higher, as NP on PEI release $0.062 \mu\text{g cm}^{-2}$ of metal cations, while NP on thiol release $0.054 \mu\text{g cm}^{-2}$ in 14 days. Release experiments performed at shorter times showed that silver cation release is relatively fast: 4.9% of total silver is released in 5 h, 7.2% in 24 h. These results are comparable with the kinetics obtained for thiol-terminated SAM.⁴

[‡] For sake of completeness, we measured the total Ag also for one preparation at 30 min, 60 min, 90 min, 2 h and 18 h dipping times, finding 1.29×10^{-6} g cm⁻², 1.43×10^{-6} g cm⁻², 1.54×10^{-6} g cm⁻², 2.08×10^{-6} g cm⁻² and 2.63×10^{-6} g cm⁻², respectively.

[§] The measured diameter of the particles in AFM images is significantly larger (25 ± 5 nm), but this is compatible with tip convolution (tips have a curvature radius of 10 nm, larger than the NP size).

[¶] The examined samples are all obtained with 15 min immersion times. In these samples, no detectable UV-Vis spectrum change was observed with respect to an Ag NP monolayer of distanced objects. In particular, it has to be remembered that by defining D = distance between adjacent particles centers and $2r$ = diameter of the particles, the ratio $D/2r$ affects significantly both the LSPR position and its lineshape when is > 5 (see ref. 26). In our case, AFM images, ICP-OES and TEM agree for a $D/2r$ = 3.3–3.5 value.

Table 1 ME values^a

	<i>S. aureus</i>		<i>E. coli</i>	
	5 h	24 h	5 h	24 h
SURF-PEI Cu	1.34	1.60	0.65	2.24
SURF-PEI Ag	1.57	0.17	1.20	1.55
SURF-PEI NP	0.03	0.86	2.57	6.16

^a Each value was obtained as an average of 3 experiments performed on different samples. $ME = \log N_C - \log N_E$ (N_C is the number of CFU/ml developed on the unmodified control glasses, N_E is the number of CFU/ml counted after exposure to a functionalized slide; CFU = colony forming unit). Tests on SURF-PEI showed $ME = 0$ against both bacterial strains.

A final comment is due about the spectral and morphological changes found at longer dipping times. Fig. 3b displays a typical AFM image for a preparation in which a large UV-Vis change (red shift and enlargement, Fig. 3d) is observed at prolonged dipping time. AFM displays dramatically enlarged NP (apparent diameter = 56.2 nm), although the increase in the average height is less important (average height = 10.1 nm). This suggests that disc-like NP form. This agrees with the observed absorption spectral changes, as for noble metal disc-like NP it has been reported that SPR displays a shorter wavelength transversal absorption and a longer wavelength longitudinal one, the latter associated to the in-plane electronic resonance.²⁴

Antibacterial activity

Table 1 shows the results of the evaluation of the microbicidal effect (ME) on functionalized glass slides. Tests were performed with an experimental procedure that simulates real life conditions of use for our modified glass slides (see Experimental). In these tests the slides are put in contact to a thin liquid film of bacterial suspension. *S. aureus* and *E. coli* were used as commonly considered representative strains for the evaluation of antibacterial activity of drugs.²⁵ Antibacterial activity was evaluated both on glasses loaded with metal ions and on glasses with silver NP. We checked ME in the 5–24 h interval, since we are interested in materials exerting a long-lasting antibacterial effect. Activity is low but not negligible for Ag⁺ and Cu²⁺ complex monolayers. This is reasonable if we consider the very small quantities of metal cations loaded on these samples (3.8×10^{-10} mol cm⁻² and 6.3×10^{-11} mol cm⁻² for Cu and Ag, respectively) and the scarce tendency of SURF-PEI to release the complexed cations (as indicated by ICP-OES).

NP-coated slides showed an efficient and long-lasting effect against *E. coli*. On the other hand, activity against *S. aureus* is poor. We recall that with the Ag NP monolayer prepared on MPTS, exerted ME effect was similar for *E. coli* ($ME = 4.93$ at 5 h and 5.90 at 24 h) but consistently stronger for *S. aureus* ($ME = 1.37$ at 5 h and 5.54 at 24 h).⁴ In both cases Ag NP are firmly grafted to the adhesive MPTS or PEI layer, and the microbicidal effect is due to slow Ag⁺ release from the NP surface. As we had already mentioned, comparing Ag⁺ release in pure water, measured by ICP-OES, discloses similar values, with a slightly larger release in the present study. This strongly suggests also that the nature of the Ag NP surface offered to the interaction of bacteria has an important role in their antibacterial effect, at least for Gram+ *S. aureus*. In this regard, it is worth mentioning that in a recent

paper,²⁷ we demonstrated that coated silver NP act with a different mechanism on Gram+ and Gram- and we observed that the coating reduces drastically the bactericidal properties of the silver NP against Gram- bacteria. Although at this stage of our research we are not able to hypothesize a mechanism for the microbiocidal effect, it can be stated that for an efficient antibacterial action *S. aureus* has to interact with a naked Ag-NP surface, even for high quantities of released Ag⁺.

Conclusions

We have demonstrated that trialkoxy-silane PEI is a low molecular weight polymer ligand suitable for surface modification and capable both of coordinating metal cations (Cu²⁺, Ag⁺) and of firmly grafting Ag-NP. Simple absorption spectroscopy techniques have been demonstrated to be useful to study the quantitative aspects of metal coordination on surface (at least for the Cu²⁺ cation). The use of a traditional analytical technique (ICP-OES) and of imaging (AFM) and optical (SE) techniques, suggests that metal cation coordination and nanoparticles grafting on surfaces may be studied with a simple and limited set of techniques, that nowadays are easily accessible in most laboratories.

The obtained metal-containing materials exert antibacterial action, that can be modulated from low to high values with moving from complexed cations to grafted nanoparticles. Moreover, we also demonstrated that coupling reactions on the primary and secondary amines in the SURF-PEI molecules is possible, at least at the less hindered centres. All of these observations strongly suggest that SURF-PEI is a versatile platform for carrying out coordination chemistry on surfaces (so far negligibly exploited), and for preparing smart, hybrid multifunctional materials, e.g. by implementing nano-objects, coordinated metal cations and organic functional components on the same surface. Studies are currently being carried on along these directions in our laboratory.

Acknowledgements

This work was supported by Fondazione Cariplo (Bandi Chiusi 2007, “Superfici vetrose ad azione antimicrobica basata sul rilascio modulato e controllato di cationi metallici”), Fondazione Alma Mater Ticinensis and “Project SAL-45” financed by Regione Lombardia.

Notes and references

- 1 E. M. Hetrick and M. H. Schoenfish, *Chem. Soc. Rev.*, 2006, **35**, 780.
- 2 (a) P. N. Danese, *Chem. Biol.*, 2002, **9**, 873; (b) K. Lewis and A. M. Klibanov, *Trends Biotechnol.*, 2005, **23**, 343; (c) A. Simchi, E. Tamjid, F. Pishbin and A. R. Boccaccini, *Nanomed.: Nanotechnol., Biol. Med.*, 2011, **7**, 22.
- 3 (a) L. Netzer and J. Savig, *J. Am. Chem. Soc.*, 1983, **105**, 674; (b) H. C. Yang, K. Aoki, H. G. Hong, D. D. Sackett, M. F. Arendt, S. L. Yau, C. M. Bell and T. E. Mallouk, *J. Am. Chem. Soc.*, 1993, **115**, 11855; (c) N. P. W. Peczonka, P. J. G. Goulet and R. F. Aroca, *J. Am. Chem. Soc.*, 2006, **128**, 12626.
- 4 P. Pallavicini, A. Taglietti, G. Dacarro, Y. A. Diaz Fernandez, M. Galli, P. Grisoli, M. Patrini, G. Santucci De Magistris and R. Zanoni, *J. Colloid Interface Sci.*, 2010, **350**, 110.
- 5 P. Pallavicini, G. Dacarro, L. Cucca, F. Denat, P. Grisoli, M. Patrini, N. Sok and A. Taglietti, *New J. Chem.*, 2011, **35**(6), 1198.
- 6 (a) S. Tan, M. Erol, A. Attygalle, H. Du and S. Sukhishvili, *Langmuir*, 2007, **23**(19), 9836; (b) M. Aslam, L. Fu, M. Su, K. Vijayamohanab and V. P. Dravid, *J. Mater. Chem.*, 2004, **14**, 1795; (c) H. Hiramatsu

- and F. E. Osterloh, *Chem. Mater.*, 2004, **16**(13), 2509; (d) D. V. Leff, L. Brandt and J. R. Heath, *Langmuir*, 1996, **12**, 4723.
- 7 (a) N. Nath and A. Chilkoti, *Anal. Chem.*, 2004, **76**(18), 5370; (b) O. P. Khatri, K. Murase and H. Sugimura, *Langmuir*, 2008, **24**, 3787; (c) R. G. Freeman, K. C. Grabar, K. J. Allison, R. M. Bright, J. A. Davis, A. P. Guthrie, M. B. Hommer, M. A. Jackson, P. C. Smith, D. G. Walter and M. J. Natan, *Science*, 1995, **267**, 1629; (d) B. S. Flavel, M. R. Nussio, J. S. Quinton and J. G. Shapter, *J. Nanopart. Res.*, 2009, **11**, 2013.
- 8 A. von Harpe, H. Petersen, Y. Li and T. Kissel, *J. Controlled Release*, 2000, **69**, 309.
- 9 (a) B. Chaufer and A. Deratani, *Nucl. Chem. Waste Manage.*, 1988, **8**, 175; (b) R. S. Juang and M. N. Chen, *Ind. Eng. Chem. Res.*, 1996, **35**, 1935; (c) R. Molinari, S. Gallo and P. Argurio, *Water Res.*, 2004, **38**, 593; (d) S. Kobayashi, K. Hiroishi, M. Tokunoh and T. Saegusai, *Macromolecules*, 1987, **20**, 1496; (e) R. Molinari, P. Argurio and T. Poerio, *Desalination*, 2004, **162**, 217.
- 10 (a) R. Sardar, J. W. Park and J. S. Shumaker-Parry, *Langmuir*, 2007, **23**, 11883; (b) C. C. Chen, C. H. Hsu and P. L. Kuo, *Langmuir*, 2007, **23**, 6801; (c) T. Mikami, Y. Takayasu and I. Hirasawa, *Chem. Eng. Res. Des.*, 2010, **88**, 1248; (d) R. Sardar, N. S. Borge and J. S. Shumaker-Parry, *Macromolecules*, 2008, **41**, 4347.
- 11 (a) A. Michna, Z. Adamczyk, M. Ocwieja and E. Bielanska, *Colloids Surf., A*, 2011, **377**, 261; (b) M. Khalid, I. Pala, N. Wasio and K. Bandyopadhyay, *Colloids Surf., A*, 2009, **348**, 263; (c) N. S. Baek, J.-H. Lee, Y. H. Kim, B. J. Lee, G. H. Kim, I.-H. Kim, M.-A. Chung and S.-D. Jung, *Langmuir*, 2011, **27**, 2717.
- 12 L. Basabe-Desmonts, J. Beld, R. S. Zimmerman, J. Hernando, P. Mela, M. F. Garcia Parajò, N. F. van Hulst, A. van den Berg, D. N. Reinhoudt and M. Crego-Calama, *J. Am. Chem. Soc.*, 2004, **126**, 7293.
- 13 (a) A. von Harpe, H. Petersen, Y. Li and T. Kissel, *J. Controlled Release*, 2000, **69**, 309; (b) F. Ungaro, G. De Rosa, A. Miro and F. Quaglia, *J. Pharm. Biomed. Anal.*, 2003, **31**, 143; (c) T. D. Perrine and W. R. Landis, *J. Polym. Sci., Part A-1*, 1967, **5**, 1993.
- 14 A. B. P. Lever and E. Mantovani, *Inorg. Chem.*, 1971, **10**, 817.
- 15 G. Albertin, E. Bordignon and A. A. Orio, *Inorg. Chem.*, 1975, **14**, 1411.
- 16 (a) C. Comuzzi, A. Melchior, P. Polese, R. Portanova and M. Tolazzi, *Eur. J. Inorg. Chem.*, 2003, 1948; (b) A. Cassol, P. Di Bernardo, R. Portanova, M. Tolazzi, G. Tomat and P. L. Zanonato, *J. Chem. Soc., Faraday Trans.*, 1990, **86**, 2841.
- 17 P. Pallavicini, G. Dacarro, M. Galli and M. Patrini, *J. Colloid Interface Sci.*, 2009, **332**, 432.
- 18 A. Moores and F. Goettmann, *New J. Chem.*, 2006, **30**, 112.
- 19 (a) E. Vandenberg, H. Elwing, A. Askendal and I. Lundstrom, *J. Colloid Interface Sci.*, 1991, **147**, 103; (b) A. Ulman, *Chem. Rev.*, 1996, **96**, 1533; (c) A. Krasnoslobodtsev and S. Smirnov, *Langmuir*, 2001, **17**, 7593; (d) A. V. Krasnoslobodtsev and S. N. Smirnov, *Langmuir*, 2002, **18**, 3181.
- 20 A. Naboka, A. Tsargorodskaya, F. Davis and S. P. J. Higson, *Biosens. Bioelectron.*, 2007, **23**, 377.
- 21 (a) S. Goubert-Renaudin, M. Etienne, S. Brandès, M. Meyer, F. Denat, B. Lebeau and A. Walcarius, *Langmuir*, 2009, **25**, 9804; (b) M. Etienne, S. Goubert-Renaudin, Y. Rousselin, C. Marichal, F. Denat, B. Lebeau and A. Walcarius, *Langmuir*, 2009, **25**, 3137.
- 22 S. Pan, Z. Wang and L. J. Rothberg, *J. Phys. Chem. B*, 2006, **110**, 17387.
- 23 A. Moores and F. Goettmann, *New J. Chem.*, 2006, **30**, 112.
- 24 (a) M. Maillard, S. Giorgio and M.-P. Pileni, *J. Phys. Chem. B*, 2003, **107**, 2466; (b) S. Chen, Z. Fan and D. L. Carroll, *J. Phys. Chem. B*, 2002, **106**, 10777.
- 25 (a) I. Sondi and B. Salopek-Sondi, *J. Colloid Interface Sci.*, 2004, **275**, 177; (b) J. Kim, *J. Ind. Eng. Chem.*, 2007, **13**, 718; (c) S. Pal, Y. K. Tak and J. M. Song, *Appl. Environ. Microbiol.*, 2007, **73**, 1712; (d) Z. Li, D. Lee, X. Sheng, R. E. Cohen and M. F. Rubner, *Langmuir*, 2006, **22**, 9820; (e) Y. Zhang, H. Peng, W. Huang, Y. Zhou and D. Yan, *J. Phys. Chem. C*, 2008, **112**, 2330; (f) K. Yliniemi, M. Vahvaselka, Y. Van Ingelgem, K. Baert, B. P. Wilson, H. Terryn and K. Kontturi, *J. Mater. Chem.*, 2008, **18**, 199; (g) S. Shrivastava, T. Bera, A. Roy, G. Singh, P. Ramachandrarao and D. Dash, *Nanotechnology*, 2007, **18**, 225103.
- 26 (a) C. L. Haynes, A. D. McFarland, L. L. Zhao, R. P. Van Duyne, G. C. Schatz, L. Gunnarsson, J. Prikulis, B. Kasemo and M. Kall, *J. Phys. Chem. B*, 2003, **107**, 7337; (b) L. L. Zhao, K. L. Kelly and G. C. Schatz, *J. Phys. Chem. B*, 2003, **107**, 7343.
- 27 E. Amato, Y. A. Diaz-Fernandez, A. Taglietti, P. Pallavicini, L. Pasotti, L. Cucca, C. Milanese, P. Grisoli, C. Dacarro, J. M. Fernandez-Hechavarria and V. Necchi, *Langmuir*, 2011, **27**, 9165.